cium fluoride at the longest wavelength (1·339 Å) which are given in Table 6. The standard deviations of these intensities calculated from counting statistics are 0·1 % and their true accuracy is estimated to be about 0·25 %. In spite of this high accuracy of measurement, which was confirmed by the reproducibility, large differences were observed between the intensities of equivalent reflexions; that between 044 and $0\bar{4}\bar{4}$ being as much as 8·6 %. Further measurements rejected non-uniformity of the beam as a possible cause and similar measurements on the strontium fluoride crystal gave excellent agreement between equivalents. These observations are therefore attributed to anisotropy in the extinction for the calcium fluoride crystal. However, since these differences occur between 180° related reflexions they must arise from variation in the perfection within the crystal and not from anisotropy of the domain shape. In order to overcome this effect one must therefore average the intensity over a suitable set of equivalent reflexions, as was done in the present analysis, and consider mean values for the domain radius and the mosaic spread parameter.

Table 6. *Neutron diffraction data for 4N reflexions from calcium fluoride at* $\lambda=1\cdot339$ Å

h k l	Intensity	$(I-I)/I$
0 2 2	251,964	+2·6%
0 $\bar{2}$ $\bar{2}$	239,378	−2·6%
4 0 0	202,006	−1·0%
$\bar{4}$ 0 0	206,155	+1·0%
4 2 2	184,138	0
$\bar{4}$ 2 2	190,903	+3·7%
4 $\bar{2}$ $\bar{2}$	179,637	−2·4%
$\bar{4}$ $\bar{2}$ $\bar{2}$	181,636	−1·3%
0 4 4	199,922	+4·3%
0 $\bar{4}$ $\bar{4}$	183,570	−4·3%
4 4 4	239,224	0
$\bar{4}$ 4 4	245,883	+2·8%
4 $\bar{4}$ $\bar{4}$	232,935	−2·6%
$\bar{4}$ $\bar{4}$ $\bar{4}$	238,470	−0·3%

Finally, we should like to emphasize that although we have obtained good agreement between the theory and experiment it is likely that some further improvement could be made in the exact form of the closed-form expressions used. It is therefore desirable that further experimental tests of this theory be carried out.

References

CHANDRASEKHAR, S., RAMASESHAM, S. & SINGH, A. K. (1969). *Acta Cryst.* A**25**, 140.
COOPER, M. J. (1970). *Acta Cryst.* A**26**, 208.
COOPER, M. J. & ROUSE, K. D. (1968). *Acta Cryst.* A**24**, 405.
COOPER, M. J. & ROUSE, K. D. (1970). To be published.
COOPER, M. J., ROUSE, K. D. & WILLIS, B. T. M. (1968). *Acta Cryst.* A**24**, 484.
HAMILTON, W. C. (1969). *Acta Cryst.* A**25**, 102.
LOOPSTRA, B. O. & RIETVELD, H. M. (1969). *Acta Cryst.* B**25**, 787.
ZACHARIASEN, W. H. (1965). *Trans. Amer. Cryst. Ass.* **1**, 33.
ZACHARIASEN, W. H. (1967). *Acta Cryst.* **23**, 558.
ZACHARIASEN, W. H. (1968*a*). *Acta Cryst.* A**24**, 425.
ZACHARIASEN, W. H. (1968*b*). *Acta Cryst.* A**24**, 324.
ZACHARIASEN, W. H. (1968*c*). *Acta Cryst.* A**24**, 212.
ZACHARIASEN, W. H. (1969). *Acta Cryst.* A**25**, 102.

Acta Cryst. (1970). A**26**, 223

Absolute Measurement of Structure Factors Using a New Dynamical Interference Effect

BY M. HART AND A. D. MILNE
H. H. Wills Physics Laboratory, University of Bristol, England

(*Received* 1 *August* 1969)

A new method of determining X-ray scattering factors by dynamical interference is described. The theoretical background to the interference effect is discussed in detail and an expression for relating the fringe period to the structure factor is developed. The method relies on anomalous transmission and is therefore most suitable for measurements on nearly perfect crystals of high atomic weight. It also has the attractive property of being insensitive to slowly varying lattice strains. Applying the method to the 220 reflexion of silicon a value of $8\cdot487\pm0\cdot017$ for the atomic scattering factor has been obtained using Mo $K\alpha_1$ radiation. This value is in excellent agreement with the author's previous results using the Pendellösung method.

1. Introduction

In recent years several attempts have been made to improve the accuracy of absolute structure factor determinations with a view to comparing the results with the values predicted by the different theoretical scattering models. With adequately precise measurements the reduction of X-ray structure factors to atomic scat-

tering factors yields too a wealth of additional information about the distribution of electrons in crystals as Dawson (1967*a*, *b*) has described.

Techniques which have been used fall into two categories: those which measure the diffracted intensity from powdered or single-crystal specimens and those which invoke dynamical interference phenomena. Although the former can be used with all materials, the accuracy of the derived structure factors is limited to between 1% and ½% (even in the most favourable cases) by the various empirical correction factors which must be applied (Miyake, 1969). Dynamical interference effects, on the other hand, are in principle capable of higher precision, mainly because the dynamical theory applies to a precisely defined physical state of the crystal whilst it is perhaps trite to remark the 'ideal powder' or the 'ideal mosaic crystal' are essentially defined theoretically in ways which do not make it clear how such artifacts can be prepared or indeed recognized from the structural point of view.

Until now only the Pendellösung interference effect has been used and several Bragg reflexions of silicon, germanium and quartz have been investigated. The relationship between structure factor and the period or order of Pendellösung fringes has been thoroughly investigated theoretically by Kato (1960, 1961*a*, *b*, 1968*a*, *b*) so that exact corrections can be made where necessary. In the most recent experiment (Hart & Milne, 1969) we have shown that by careful optimization of the variable parameters and by the strict elimination of correction factors, statistical errors of less than 0·1% can be achieved in Pendellösung experiments using two radiations and three different specimens. The method, however, lays very stringent conditions on the behaviour of the X-ray wavefields inside the crystal and this restricts its use to single crystals of almost perfect material.

Another interference effect, produced by a non-diffracting zone in a crystal, has also been examined in detail (Milne, 1966; Authier, Milne & Sauvage, 1968) and is here developed as a second dynamical interference method of structure factor measurement. It is in principle quite different from the Pendellösung method since only one branch of the dispersion surface is active whereas, in the Pendellösung method, interference is observed between waves from two separate branches of the dispersion surface. At this stage it is important that these two *different* methods exist, for correlation between results is strong evidence of there being no significant systematic errors.

The problem of systematic errors is of course no less serious in structure factor determinations than in any other measurements. In particular, the Pendellösung method is susceptible to systematic errors if the crystal is distorted either by grown-in defects or by elastic strain. It seems likely that the discrepancies between previously published results using that method are due, at least in part, to undetected lattice distortion. In this connexion we stress again that, before serious work is started, adequately sensitive diffraction topography of the crystal must be carried out. If the strain distribution is sufficiently simple it may be possible to chose diffraction conditions such that the strain is harmless (Hart & Milne, 1969). In our experience no crystals which we have examined are sufficiently perfect that their internal strains can be *ignored* in Pendellösung

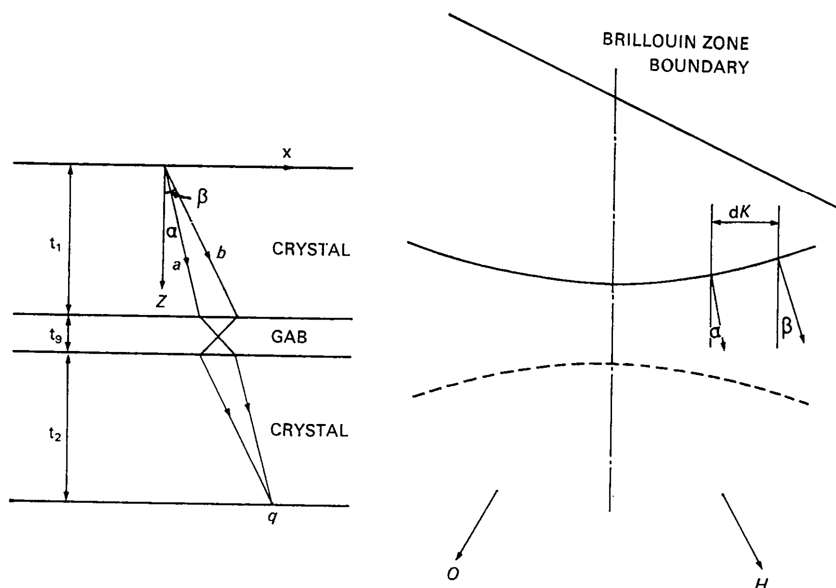

Fig. 1. Geometrical quantities in real space (left) and reciprocal space (right) used in the calculation of the interference patterns of a crystal containing a gap.

measurements of structure factors. An important feature of the present method is that it is insensitive to strains which have only slow spatial variations.

In this paper a measurement of the 220 structure factor of silicon using interference fringes formed in a crystal containing a non-diffracting zone will be described.

2. Theory

In general the diffraction contrast produced by a thin non-diffracting lamella in an otherwise perfect crystal can be explained by considering the interference of the eight plane-wave components of the incident, linearly polarized, spherical wave which pass through each point on the exit surface of the crystal (Authier, Milne & Sauvage, 1968). In sufficiently thick crystals however, where one of the wavefields is highly attenuated by the Borrmann effect (Borrmann, 1941, 1950), the situation is considerably simplified and only two plane wave components need be considered for each polarization state. For transmission in the symmetric case, which will be considered exclusively, two such waves which intersect the exit surface at q (Fig. 1) having travelled along paths a and b, can be described by

$$D_a = D(t_1+t_2)^{-1/2} f_1(\Delta\theta) \exp[-i(\varphi_0 - \pi/2)]$$
$$D_b = D(t_1+t_2)^{-1/2} f_2(\Delta\theta) \exp[-i(\varphi_h - \pi/2)] \quad (1)$$

where D is a constant related to the incident wave, t_1 and t_2 are the thicknesses of the diffracting regions on either side of the lamella, and $f_1(\Delta\theta)$ and $f_2(\Delta\theta)$ describe the variation of amplitude with the angle of incidence.

The phase terms φ_0 and φ_h are given by

$$\varphi_0 = \frac{\pi}{\Delta_0}(t_1+t_2)(1-P_\alpha^2)^{1/2}$$
$$\varphi_h = \frac{\pi}{\Delta_0}(t_1+t_2)(1-P_\beta^2)^{1/2} \quad (2)$$

where

$$\Delta_0 = \frac{\lambda \cos\theta}{C(\chi_h\chi_{\bar{h}})^{1/2}} \quad (3)$$

and P_α and P_β are deviation parameters defined in terms of the angles α and β by

$$\left.\begin{aligned} P_\alpha &= \tan\alpha / \tan\theta \\ P_\beta &= \tan\beta / \tan\theta \end{aligned}\right\} . \quad (4)$$

χ_h and $\chi_{\bar{h}}$ are the hkl and $\bar{h}\bar{k}\bar{l}$ coefficients in the Fourier expansion of the dielectric susceptibility χ. To an accuracy of 0·1% for low order Bragg reflexions in silicon they are related to the structure factor F_h by the relationship

$$(\chi_h\chi_{\bar{h}})^{1/2} = \frac{r_e\lambda^2}{\pi V}|F_h| , \quad (5)$$

where r_e is the classical electron radius, V is the volume of the unit cell, λ is the X-ray wavelength and θ is the Bragg angle. The polarization factor C, takes the values 1 in the σ case when the electric vector of the incident wave is at right angles to the plane defined by the wave vectors for the incident and diffracted beams and $|\cos 2\theta|$ for the π case when the electric vector is normal to that plane.

If the thickness t_g of the non-diffracting zone is much less than the total crystal thickness (t_1+t_2), the two paths a and b are nearly parallel inside the crystal and the phase difference δ_{ab} at q between the two interfering waves is given by

$$\delta_{ab} = \mathrm{Re}(\varphi_0 - \varphi_h) . \quad (6)$$

This phase difference can be expressed in terms of an average value $\bar{P}$ of the deviation parameter. To an accuracy of 0·1% we can write

$$\delta_{ab} = \frac{2\pi}{\Delta_0} t_g \bar{P}(1-\bar{P}^2)^{-1/2} = 2\pi n_0 , \quad (7)$$

where

$$\bar{P} = \tfrac{1}{2}(P_\alpha + P_\beta) = \tan\Lambda / \tan\theta \quad (8)$$

and n_0 is called the order of interference.

Hence, if the crystal and lamella thicknesses are known, the structure factor can be obtained directly by measuring the interference order as a function of position on the exit surface of the crystal.

Polarization

With an unpolarized source of X-rays the observed interference pattern is complicated owing to the superposition of the patterns produced by the two polarization components of the incident wave. As the intensity and period of the fringe patterns are different for the two states of polarization it is not possible to describe the observed pattern with sufficient accuracy in terms of an average polarization factor. However, a good approximation to the position of the experimentally obtained fringes can be calculated theoretically. If we write the diffracted intensity I_h to show explicitly the two components we have

$$I_h \propto A\cos^2\left[\frac{\pi}{\Delta_0^\sigma} t_g \bar{P}(1-\bar{P}^2)^{-1/2}\right] + B\cos^2\left[\frac{\pi}{\Delta_0^\sigma}|\cos 2\theta|\, t_g \bar{P}(1-\bar{P}^2)^{-1/2}\right] \quad (9)$$

where Δ_0^σ denotes the value of Δ_0 corresponding to the σ case of polarization, obtained by substituting $C=1$ in equation 3. The factors A and B allow for the difference in attenuation and scattering of the two polarization components and are given by

$$A = \exp(-\mu^\sigma t) \quad \text{and} \quad B = |\cos 2\theta| \exp(-\mu^\pi t) \quad (10)$$

where $t = t_1 + t_2$ is the thickness of the crystal and μ^σ and μ^π are absorption coefficients approximately given

by

$$\mu^\sigma = \mu_0 \frac{\cos A}{\cos \theta} \left[1 - \frac{\chi_{ih}}{\chi_{i0}} (1 - \bar{P}^2)^{1/2}\right]$$

$$\mu^\pi = \mu_0 \frac{\cos A}{\cos \theta} \left[1 - |\cos 2\theta| \frac{\chi_{ih}}{\chi_{i0}} (1 - \bar{P}^2)^{1/2}\right]. \qquad (11)$$

μ_0 is the normal linear absorption coefficient, A is defined by equation (7) and χ_{i0} and χ_{ih} are the imaginary parts of χ_0 and χ_h respectively.

The attenuation coefficients given in equation (11) are not related to *actual* trajectories of the interfering waves. Although the phase difference can be expressed in terms of an average deviation parameter $\bar{P}$, the attenuation of the interfering waves is not simply related to $\bar{P}$ but to the specific values of P_α and P_β. Towards the edge of the patterns, at large deviations from the exact Bragg angle, the introduction of $\bar{P}$ instead of P_α and P_β is quite justified but close to the centre of reflexion where the two tie points α and β lie on opposite sides of the Brillouin zone boundary our attenuation coefficients are systematically too large.

Because we have chosen to use quite thick anomalously transmitting crystals $[\mu_0(t_1+t_2) \simeq 10]$ the polarization ratio A/B is large near the centre of the reflecting range so that there the observed pattern is nearly a pure σ case pattern and the correction due to the second term in equation (9) is small. As we mentioned before, towards the edge of the observed fringe patterns where the polarization ratio approaches $|\cos 2\theta|$ the mean Poynting vector approximation (equation 11) is a good one. Because the observed pattern is predominantly formed with σ-polarized radiation it is experimentally convenient to compare equation (9) with the test function I defined in equation (12)

$$I^\sigma \propto A \cos^2 \left[\frac{\pi}{\Delta_0^\sigma} t_g \bar{P}(1 - \bar{P}^2)^{-1/2}\right]. \qquad (12)$$

The extrema of the test function I^σ occur for integral values m of the argument. It is straightforward to show that the corresponding extrema of the observed pattern I_h are shifted by an amount δm where

$$\sin (2\pi\delta m) = \cos^2 2\theta \exp \left[- \mu_0 t(1 - |\cos 2\theta|) \frac{\cos A}{\cos \theta} \times (1 - \bar{P}^2)^{1/2} \frac{\chi_{ih}}{\chi_{i0}}\right] \times \sin \left[\frac{2\pi}{\Delta_0^\sigma} t_g |\cos 2\theta| \bar{P}(1 - \bar{P}^2)^{-1/2}\right]. \qquad (13)$$

Because only a few fringes are visible we cannot chose to make δm zero so that the shift of each fringe has to be calculated from equation (13).

Crystal perfection

We have so far assumed that the crystal is ideally perfect. Of course we can ensure that only crystals which are free of planar defects and dislocations are used but cannot, in silicon which is commercially available, avoid point to point variations in lattice parameter. Sensitivity to strain occurs at two levels in these experiments: X-ray energy flow may be modified by the strain in each crystal wafer or, more sensitively, moiré effects between the two parts of the crystal may become troublesome.

In weakly strained crystals the tie-points which characterize waves in the crystal migrate along the dispersion surface so that the wavefield accommodates itself to the *local* lattice (Penning & Polder, 1961; Kato, 1964; Bonse, 1964; Hart & Milne, to be published). If the strain field is homogeneous then all tie-points move so that the change in the component of wave vector parallel to the local diffraction vector, $\Delta\mathbf{K}_x$, is a constant and

$$\Delta\mathbf{K}_x = \frac{p}{2\Delta_0 \tan \theta} \qquad (14)$$

where

$$p = \frac{2 \tan \theta \, \Delta_0}{\lambda \cos \theta} \left[\cos^2 \theta \frac{\partial^2 U}{\partial z^2} - \sin^2 \theta \frac{\partial^2 U}{\partial x^2}\right]. \qquad (15)$$

$U(x, z)$ is the atomic displacement function for the imperfect crystal.

Even in the best crystals available this tie-point migration can be an important source of systematic error in Pendellösung experiments (Hart & Milne, 1969). However, in the present experiments, weak deformations (for which $\partial^2U/\partial x^2$ and $\partial^2U/\partial z^2$ are constant over the volume of crystal contributing to the diffracted beam) have little influence on the observed fringe spacing. If we expand equation (7) to first order in $\bar{P}$ the fringe spacing Δ is constant and given by

$$\Delta = \Delta_0(t_1 + t_2) \tan \theta / t_g . \qquad (16)$$

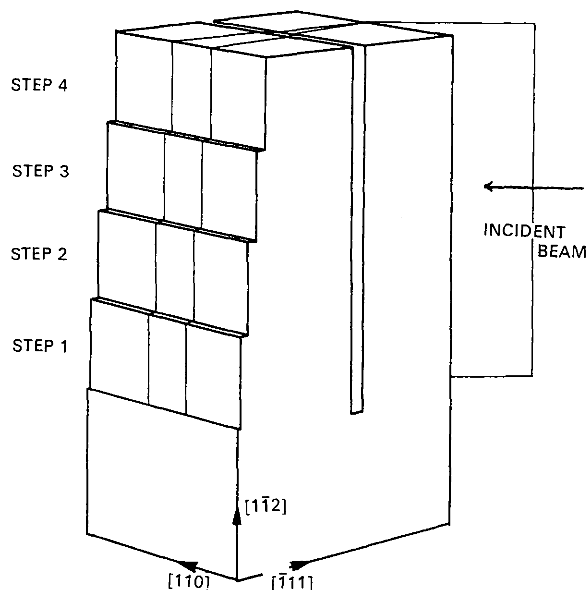

Fig. 2. Orientation and design of the stepped crystal.

Straightforwardly one can show that $\Delta=|dK|^{-1}$ (Fig. 1) where dK is the separation of the tie points measured in the direction parallel to the diffraction vector. In a homogeneous strainfield ΔK_x is the same for all waves so that dK, and hence Δ, is not changed by weak deformations of the crystal.

Because these fringes are spherical wave moiré fringes their phase is affected by translations of one part of the bicrystal with respect to the other. This is simply a change in the phase of the lattice in the second part of the crystal with respect to the waves in the gap. The phase change is $2\pi\mathbf{h}\,.\,\mathbf{f}$ where $\mathbf{f}$ is the translation vector of the two crystal lattices. Referring our equations to an origin in the first crystal changes equation (7) to

$$n_0+\varepsilon=n_0+\mathbf{h}\,.\,\mathbf{f}=\frac{t_g}{\Delta_0}\bar{P}(1-\bar{P}^2)^{-1/2} \qquad (17)$$

so that the centre of the observed pattern need not be an interference maximum.

3. Experimental considerations

According to equation (17) the fringe position is very sensitive to relative shifts between the two diffracting elements: $\mathbf{h}\,.\,\mathbf{f}=0{\cdot}1$ when $|f|=10^{-9}$ cm if $|h|^{-1}=10^{-8}$ cm. To achieve the necessary stability we have made measurements on a block of silicon containing an appropriate narrow groove rather than on pairs of crystals separated by a narrow gap.

As in our Pendellösung experiments we have made measurements on Lopex silicon grown in the [$\bar{1}$11] direction by Texas Instruments. Although the present fringe systems are insensitive to strain we have chosen to measure the 220 Bragg reflexion so that the intrinsic crystal strains are harmless [$p=0$ in equation (14)]. So that the fringe system could be studied easily over a wide range of the adjustable parameters a stepped sample was prepared (Fig. 2). The crystal orientation was determined to better than 1 min of arc and the specimen cut with a high speed diamond-edged slitting saw. The X-ray entrance surface, gap, and stepped surface were all cut without removing the crystal from its mount so that all of these surfaces were precisely parallel to one another and within 1 min of arc of the ($\bar{1}$11) plane. Surface damage introduced during crystal cutting was afterwards removed by chemical polishing.

Specimen dimensions

Experimentally the fringe spacing Δ and the specimen dimensions $[t_1+t_2]$ and t_g are the only quantities measured [see equations (3), (4), (5), (7), (8), or, more simply equation (16)]. There are no ideal specimen dimensions but the optimum size is dictated by a number of considerations.

The specimen surfaces are not smooth to better than 1–2 μm so that the gap must be of order 500 μm if we are to measure its width to 0·2%. On the other hand the gap must not be so wide that the coherent wavefields can become spatially separated in the second part of the crystal.

The crystal thickness must be so large that the contribution of the strongly absorbed wavefields is negligible. At the centre of the range of Bragg reflexion for the σ case of polarization in the 220 Bragg reflexion of Mo $K\alpha_1$ radiation from silicon, this contribution is 1% of the intensity at a crystal thickness of 3·5 mm. The situation is much less favourable for Ag $K\alpha_1$ radiation and for other angles of incidence. In practice we were limited to a total specimen thickness $[t_1+t_2]$ of about 8 mm by intensity considerations. This, too, determined the collimator slit width which was approximately 10 μm.

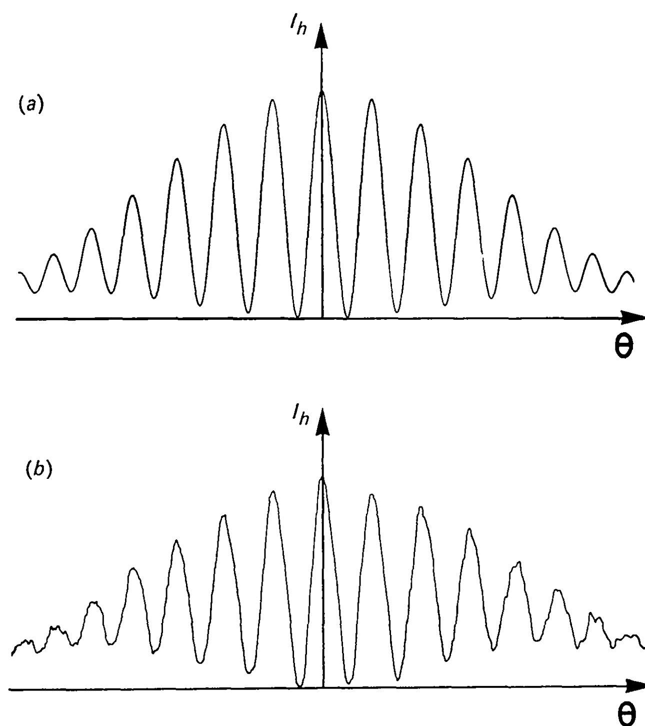

Fig. 4. Comparison between (*a*) the theoretical fringe pattern calculated from equation (9) and (*b*) a microdensitometer trace of step 2 of Fig. 3(*a*) obtained with Mo $K\alpha_1$ radiation.

4. Experimental method

The specimen was mounted on a slide unit with the well collimated ribbon beam of X-rays incident at the Bragg angle for the 220 Bragg reflexion. Interference topographs were recorded on nuclear emulsion plates (Ilford type L4 – 50 μm) using Mo $K\alpha_1$ and Ag $K\alpha_1$ radiations at three positions 0·5 mm apart in the specimen. A typical pair of interference patterns obtained from the stepped crystal sketched in Fig. 2 is shown in Fig. 3. In Fig. 4 a direct qualitative comparison is made between the theoretical fringe profile calculated from equation (9) and a densitometer trace of one of

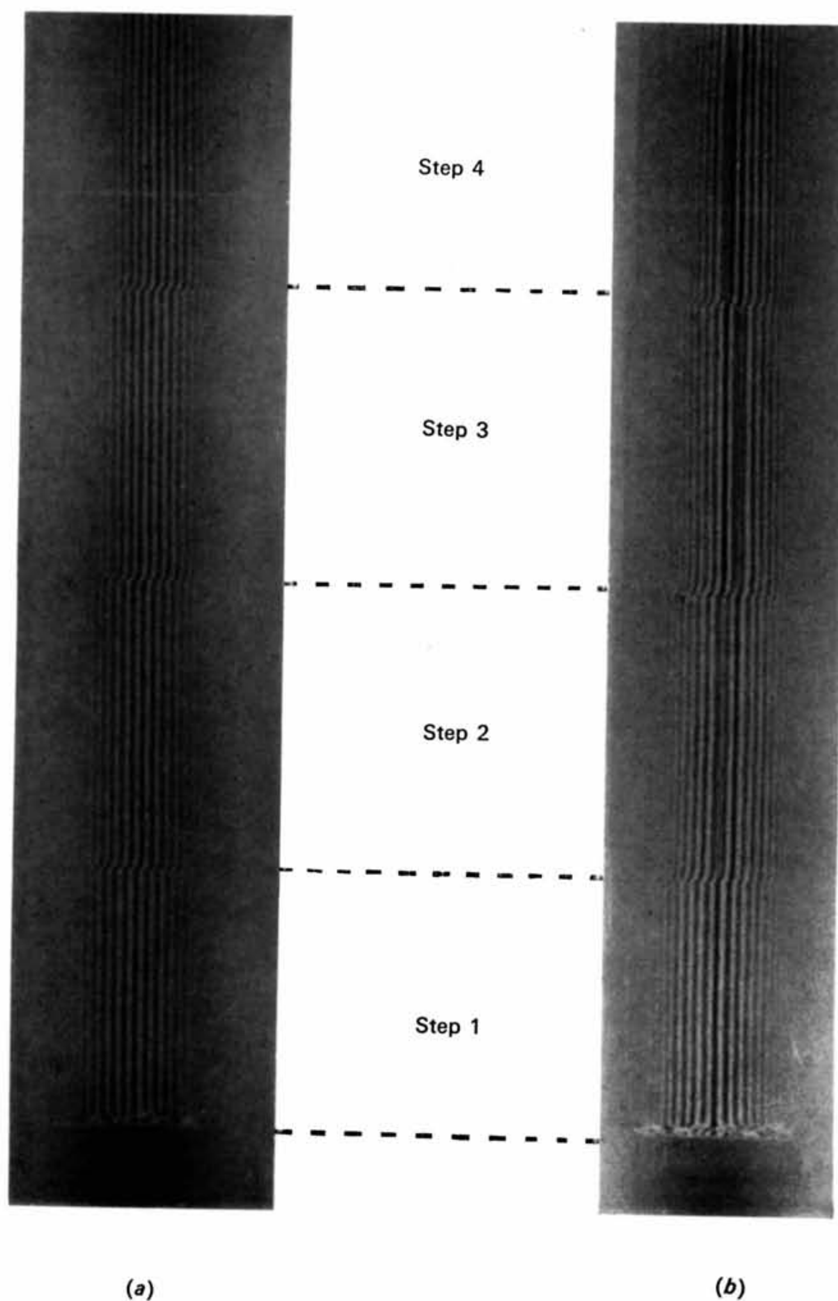

Fig. 3. Interference fringe patterns obtained from the sample sketched in Fig. 2 using (*a*) Mo $K\alpha_1$ and (*b*) Ag $K\alpha_1$ radiation.

the steps in Fig. 3(*a*). Evidently the theoretical approximation used to derive equation (9) is satisfactory over the range of $\bar{P}$ involved in these experiments.

When the X-ray experiments were completed the specimen was cut parallel to the Bragg planes at the positions where interference patterns had been obtained. The thicknesses of the specimen and gap were then measured directly with a travelling microscope.

5. Results

Fortunately it is not necessary to obtain values of the structure factor by computing a theoretical fringe pattern and comparing that with a microdensitometer trace of an experimental pattern. An exact version of equation (9) can of course be straightforwardly derived but curve fitting would involve at least three adjustable parameters F_h, χ_{ih}/χ_{io} and ε. Using the facts that $\bar{P}<0{\cdot}5$ and that the observed pattern is almost σ-polarized we have instead used a linear graphical method to derive a value of F_h from the observed patterns. In the absence of interference fringes I_h is symmetric in the deviation parameter $\bar{P}$. We can therefore locate the position in the interference pattern where $\bar{P}=0$ because it is the line of symmetry of the envelope of the fringe intensity pattern. Since, in a typical case $t_g/\Delta_0\simeq 10$ and the origin of $\bar{P}$ could be determined to about 0·1 fringes, the absolute error in $\bar{P}$ was 0·01. Thus, even with $\bar{P}=0{\cdot}5$ the error in $(1-\bar{P}^2)^{-1/2}$ is only just over 0·1 %. If we calculate $\bar{P}(1-\bar{P}^2)^{-1/2}$ for every fringe, the gradient $G=\frac{d}{dn_0}[\bar{P}(1-\bar{P}^2)^{-1/2}]$ can still be evaluated to within 0·1 %. At the same time a correction for the fringe shift δm caused by the π-polarized waves can be made. An example of the calculation for one step on a Mo $K\alpha_1$ fringe pattern is shown in Table 1. From these results the gradient G was calculated by the method of least squares.

Since

$$G=\Delta_0^\sigma/t_g \tag{7}$$

and

$$\bar{P}=x/(t_1+t_2)\tan\theta\,, \tag{8}$$

where x is the distance measured along the exit surface of the crystal (Fig. 1), values of Δ_0^σ can be straightforwardly calculated. A complete set of results is collected in Table 2.

Table 1. *Sample calculations for step* 2 *at position A on the* Mo $K\alpha_1$ *pattern of Fig.* 3

Order m	$\bar{P}$	$\bar{P}(1-\bar{P}^2)^{-1/2}$	δm
5	0·350	0·371	0·065
4	0·287	0·301	0·068
3	0·221	0·227	0·061
2	0·148	0·150	0·039
1	0·074	0·074	0·011
0	−0·002	−0·002	0·000
−1	−0·075	−0·075	−0·011
−2	−0·150	−0·152	−0·039
−3	−0·221	−0·227	−0·061
−4	−0·287	−0·300	−0·068
−5	−0·349	−0·373	−0·065

There are no obvious systematic trends in the table of results and the mean values are

$$\Delta_0^\sigma=36{\cdot}44\ \mu\text{m}\pm 0{\cdot}07\ \mu\text{m for Mo } K\alpha_1$$
$$\Delta_0^\sigma=46{\cdot}48\ \mu\text{m}\pm 0{\cdot}07\ \mu\text{m for Ag } K\alpha_1\,.$$

Using equations (3) and (5) we find:

$$f=8{\cdot}487\pm 0{\cdot}017 \text{ for Mo } K\alpha_1 \tag{18a}$$
$$f=8{\cdot}494\pm 0{\cdot}013 \text{ for Ag } K\alpha_1\,. \tag{18b}$$

Table 2. *Complete set of results*

(t_1+t_2) measured in mm, t_g and $\Delta_0{}^\sigma$ are measured in μm.

			Mo $K\alpha_1$		Ag $K\alpha_1$	
Position *A*	(t_1+t_2)	t_g	G	$\Delta_0{}^\sigma$	G	$\Delta_0{}^\sigma$
Step 1	7·974	487	0·07460	36·33	0·09489	46·21
Step 2	7·652	492	0·07388	36·35	0·09486	46·67
Step 3	7·311	492	0·07362	36·22	0·09366	46·08
Step 4	6·960	492	0·07356	36·19	0·09476	46·62
	Mean $\Delta_0{}^\sigma$		36·27 ± 0·04		46·40 ± 0·13	
Position *B*						
Step 1	7·977	494	0·07427	36·69	0·09496	46·91
Step 2	7·653	496	0·07407	36·74	0·09419	46·72
Step 3	7·306	497	0·07348	36·52	0·09352	46·48
Step 4	6·956	498	0·07438	37·04	0·09450	47·06
	Mean $\Delta_0{}^\sigma$		36·75 ± 0·10		46·71 ± 0·11	
Position *C*						
Step 1	7·972	489	0·07392	36·15	0·09481	46·36
Step 2	7·651	493	0·07363	36·30	0·09422	46·45
Step 3	7·308	494	0·07348	36·30	0·09370	46·29
Step 4	6·957	494	0·07387	36·49	0·09443	46·65
	Mean $\Delta_0{}^\sigma$		36·31 ± 0·06		46·44 ± 0·07	

These results are experimental values at 20°C with no corrections for thermal motion or anomalous dispersion and should be compared with our previous results which were obtained by the Pendellösung method. They are

$$f=8{\cdot}478 \pm 0{\cdot}008 \text{ for Mo } K\alpha_1 \qquad (19a)$$

$$f=8{\cdot}448 \pm 0{\cdot}012 \text{ for Ag } K\alpha_1\,. \qquad (19b)$$

Remembering that the gap crystal was designed for Mo $K\alpha_1$ radiation and not specifically for Ag $K\alpha_1$ the above agreement is very encouraging.

6. Discussion

The primary source of random error lies in the determination of the gap width. Because the crystal surfaces must all be chemically polished to remove handling strains and surface damage, we were not able to determine t_g to better than 0·2% and this error is propagated, almost without change, into the final scattering factors.

Although we were able to ensure that residual crystal strains had no influence on wavefield propagation some moiré fringe shifts were observed. The order shift ε varied from step to step and from one position to the next, but was effectively eliminated by the graphical method outlined in § 5. This approach is justified by the internal consistency of the results in Table 2. Potentially the most awkward feature of the experiment is the problem of X-ray polarization. The *ad hoc* approach adopted here has the great advantage of simplicity. It is important to notice, that because the polarization ratio A/B is large in these anomalous transmission experiments, the fringe shifts due to π-polarized waves are small (Table 1) causing approximately a 2% change in G. In the least-squares line fitting used to determine G the outer fringes have greatest weight and those are the fringes for which the approximate treatment of polarization [equations (10) and (11)] should be most reliable.

Finally, we would comment on a misunderstanding which arose in the discussion at the Cambridge meeting (Hart & Milne, 1969) concerning the systematic difference between the silicon scattering factors measured with Mo $K\alpha_1$ and Ag $K\alpha_1$ radiations (19*a*, *b*) using the Pendellösung fringe method. As Dr B. Dawson has since pointed out to us, the observed difference is exactly that predicted by theories of anomalous dispersion. For example, using Hönl's (1933*a*, *b*) equations one calculates $\Delta f'(\text{Mo } K\alpha_1) - \Delta f'(\text{Ag } K\alpha_1) = 0{\cdot}035$ for the K electrons of silicon whereas we measured $f(\text{Mo } K\alpha_1)/f(\text{Ag } K\alpha_1) = 1.0035 \pm 0{\cdot}0007$ or $f(\text{Mo } K\alpha_1) - f(\text{Ag } K\alpha_1) = 0{\cdot}030 \pm 0{\cdot}006$. Bearing in mind that the present experiments were performed under optimum conditions only for Mo $K\alpha_1$ radiation, we consider that the present Ag $K\alpha_1$ measurement (18*b*) is subject to systematic error and that the other results are mutually consistent. This opinion is supported too by the patterns obtained in Fig. 3(*b*). Not only are there important intensity contributions from the strongly absorbed wavefields but also margin enhancement (Kato, 1960) can be clearly seen in the Ag $K\alpha_1$ patterns. It is therefore not too surprising that the results deduced from the Ag $K\alpha_1$ patterns are systematically different from those derived from the Mo $K\alpha_1$ patterns. Nevertheless, the total spread in all of our results to date, obtained by two independent methods, is still only $\pm\frac{1}{4}$%.

Although, for weakly absorbing crystals, this new method is generally inferior to the Pendellösung method, there are several situations in which it assumes some importance. It provides *independent* support for the structure factors which we have measured previously by the Pendellösung technique. There are no other interference methods which can be very accurately applied to strongly absorbing crystals like germanium, for which the present method is ideally suited.

This work was supported in part by the Science Research Council.

References

AUTHIER, A., MILNE, A. D. & SAUVAGE, M. (1968). *Phys. Stat. Sol.* **26**, 469.
BONSE, U. (1964). *Z. Phys.* **177**, 385.
BORRMANN, G. (1941). *Z. Phys.* **42**, 157.
BORRMANN, G. (1950). *Z. Phys.* **127**, 297.
DAWSON, B. (1967*a*). *Proc. Roy. Soc.* A**298**, 255.
DAWSON, B. (1967*b*). *Proc. Roy. Soc.* A**298**, 379.
HART, M. & MILNE, A. D. (1969). *Acta Cryst.* A**25**, 134.
HÖNL, H. (1933*a*). *Z. Phys.* **84**, 1.
HÖNL, H. (1933*b*). *Ann. Phys.* **18**, 625.
KATO, N. (1960). *Z. Naturf.* **15**a, 369.
KATO, N. (1961*a*). *Acta Cryst.* **14**, 526.
KATO, N. (1961*b*). *Acta Cryst.* **14**, 627.
KATO, N. (1964). *J. Phys. Soc. Japan*, **19**, 67.
KATO, N. (1968*a*). *J. Appl. Phys.* **39**, 2225.
KATO, N. (1968*b*). *J. Appl. Phys.* **39**, 2231.
MILNE, A. D. (1966). M.Sc. Thesis, University of Bristol.
MIYAKE, S. (1969). *Acta Cryst.* A**25**, 257.
PENNING, P. & POLDER, D. (1961). *Philips Res. Repts.* **16**, 419.